Volume 3, Issue 3 (2015) 478- 489 ISSN 2347 - 3258
International Journal of Advance Research and Innovation

An Investigation for Evaluating Distinct Test Functions for Predicting Elastic Deformations of Metal Parts Using

Ajay Chhillar *, Rajender Singh
Department of Mechanical Engineering, DCRUST Murthal, Sonipat, Haryana, India

Article Info

Article history:
Received 05 July 2015
Received in revised form
20 July 2015
Accepted 28 August 2015
Available online 15 September 2015

Keywords

Modified Meshless Method,
Meshless Local Petrov Galerkin (MLPG) Method, Moving Least Square (MLS) method, Test function,
Elastic deformation

Abstract

Elastic deformation of metal parts has been a matter of great concern for investigation of researchers in academia and research institutions all over the world. Literature reveals that earlier researchers have applied efforts for evaluating Gaussian and spline test functions only for predicting elastic deformations. However few research efforts have been reported in literature for predicting elastic deformation through modified meshless method using exponential test functions. This paper presents an investigation for evaluating distinct test function for predicting elastic deformations of metal parts using modified meshless method. In present work, a modified meshless method has been implemented with three distinct test functions namely Gaussian, Exponential and Spline both with linear and quadratic basis function. Results of investigation reveal that Gaussian test function provides accurate results followed by exponential and spline functions. Effect of choosing different geometrical parameters affecting the solution for prediction of elastic deformation in case of exponential test function has also been presented here. Moreover, the present investigation for evaluating distinct test functions for predicting elastic deformations of metal parts using modified meshless method helps to observe that computational results with higher order basis functions are almost ten times better when compared with lower order basis functions.

1. Introduction

Elastic deformation of metal parts has been important activity in the area of solid mechanics. Numerous techniques were used to find elastic deformation of metal parts which has been a matter of great concern for investigators all over the world. For last few decades many researchers have been reported to work on meshless methods for alleviating the major drawbacks of Finite Element Methods (FEM) [**1**], [**2**], [**3**], [**4**], [**5**], [**6**], [**7**], [**8**], [**9**], [**10**]. The research scholars working on Meshless methods criticize the FEM for the grid requirement for integration and domain representation. The pioneers working in meshless field adopted some fine features of FEM and they generated the system equations of the physical phenomena over the nodes without any grids formation. The first meshless technique named as Smooth Particle Hydrodynamics (SPH) method [**11**] was reported in literature in the year 1977 for solving fluid flow problems. However, this method could not be much admired by other researchers. The leap and bound progress in the area of meshless methods took place after the Diffuse Element Method (DEM) [**12**] in the year 1992. Afterwards within a short span of time, more number of meshless methods were reported in literature namely Element Free Galerkin (EFG) Method in 1994 [**13**], Boundary Node Method (BNM) [**14**], Reproducing Kernel Particle Method (RKPM) [**15**], hp-Meshless Cloud Method [**16**], Finite Pont Method (FPM) [**17**], Meshless Local Petrov Galerkin (MLPG) Method [**18**], Finite Spheres Method [***19***], Local Boundary Integral Equation (LBIE) Method [***20***], Point Interpolation Method (PIM) [***21***], Gradient Smoothing Method [***22***], Finite Mass Method [***23***], Radial Point Interpolation Based Finite Difference Method [***24***]. Local Maximum-Entropy (LME) [***25***], Local Kriging (lokriging) Method [***26***], Generalized Meshfree Approximation (GMF) [***27***], Discrete Least Square Meshless Method (DLSM) [***28***], Radial Basis Integral Equation Method [***29***]. Truly Meshless Point Weighted Least Squares (PWLS) Method [***30***], Repeated Replacement Method (RRM) [***31***], variation of Local Point Interpolation Method (vLPIM) [***1***], Random Differential Quadrature (RDQ) Method [***1***]. Literature reveals that earlier researchers have applied efforts for evaluating Gaussian, and spline test functions only for predicting elastic deformations of metal parts. In the present study, very few research efforts have been reported in literature for predicting elastic deformation of metal parts through modified meshless method using exponential test functions both with linear and quadratic basis function. This paper presents an investigation for evaluating distinct test function for predicting elastic deformations of metal parts using modified meshless method. In the present study, a modified meshless method has been implemented with three distinct test functions, namely Gaussian, Exponential and Spline functions both with linear and quadratic basis function.

Most of the above listed meshless methods need grids formation either for interpolation or for integration reasons. These Meshless methods are not truly meshless. However, there are some other meshless methods which neither require any grid formation for integration nor for interpolation reasons. Such methods are popularly known as truly meshless methods. In the year 2005, Atluri and Shengping [***32***] stated that MLPG method is a concept and some other meshless methods can be devised from this method by suitable choice of test and trial functions. The present work emphasizes on the performance analysis of exponential test function for solving elastostatic problems

Corresponding Author,
E-mail address: aasc1981@gmail.com

though a truly meshless approach. This truly meshless approach utilizes the Moving Least Square Approximation Scheme (MLSAS) for approximating field variables and the same is presented as under.

2. Moving Least Square Approximation Scheme

The MLSAS approach consider 1-D problem domain where Schematic representation of Error e_i for a field node 'i', support domain of a node 'x', domain of definition of point 'y', weight function for 1-D case of MLSAS in meshless method is presented in Fig. 1. Where Ω_s^x represents sub-domain of node x. To compute the distribution of u inside sub-domain Ω_s^x containg randomly located nodes $\{x_i\}$, $i = 1, 2, 3, \ldots n$, the MLS approximant of field variable represented as $u^h(x)$ is presented by Salkauskas and Lancaster [33] as

$u^h(x) = P^T(x)\, a(x) = \sum_j^m p_j(x)\, a_j(x) \; \forall x \in \Omega_s^x$ (1)

Where $\mathbf{P^T(x)} = [\mathbf{p_1(x)}, \mathbf{p_2(x)}, \mathbf{p_3(x)}, \ldots \mathbf{p_m(x)}]$ is a set of basis functions of order **m** according to Pascal's **[**5**]** for completeness of the basis function. And $\mathbf{a(x)}$ is vector of unknown coefficients. The vector $\mathbf{a(x)}$ can be computed through two approaches according to Breitkopf et al **[**34**]** **[**35**]**. The minimization of weighted discrete $\mathbf{L_2}$ norm is applied to determine vector $\mathbf{a(x)}$ using Eq. (2) in matrix form

$$J(x) = [P.a(x) - \hat{u}]^T .W.[P.a(x) - \hat{u}] \qquad (2)$$

Where [P] is polynomial basis function vector, [W] is weight function matrix and the functional J(x) represents weighted square error. Now differentiating Eq. (2) with respect to unknown coefficient vector $a(x)$ and equating it to zero, the least square error will be then minimized.

$$\frac{\partial J}{\partial a(x)} = 0 \qquad (3)$$

The stationarity of J(x) functional in Eqs. (2) with respect to $a(x)$ will give the following set of linear equations between unknown coefficient vector $a(x)$ and actual field variable $\hat{u}$.

$$A(x)a(x) = B(x)\hat{u} \qquad (4)$$

Now solving for unknown coefficient vector $a(x)$ from Eq. (4) and on substituting it in Eq. (1), will give Eq. (5). The similar function is also used in FEM.

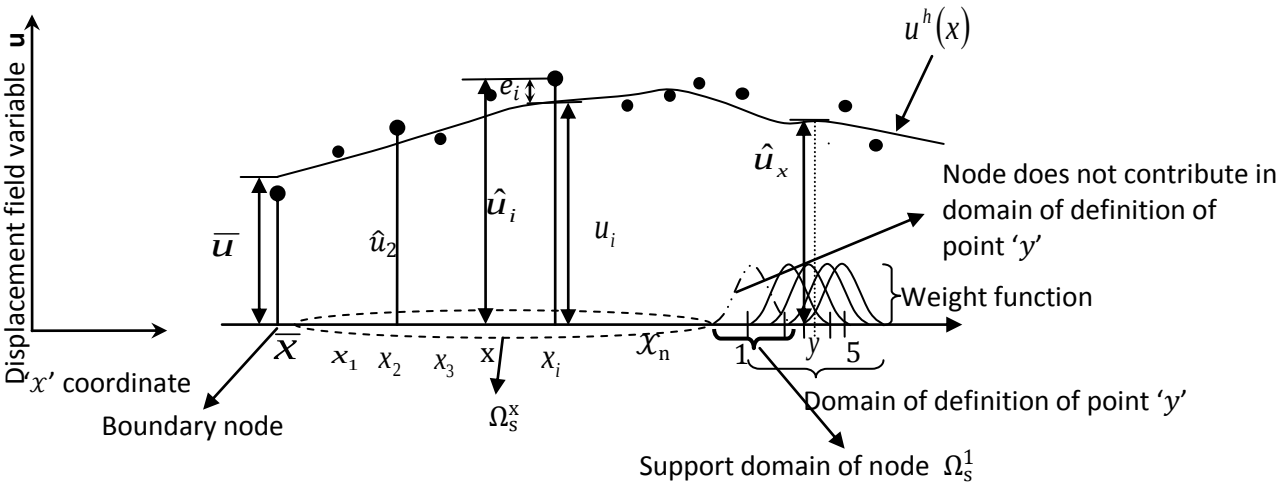

Figure 1- Schematic representation of Error e_i for a field node 'i', support domain of a node 'x', domain of definition of point 'y', weight function for 1-D case of MLSAS in meshless method.

$$u^h(x) = \phi^T(x).\hat{u} = \sum_{i=1}^{n} \phi_i(x).\hat{u}_i \; ; \qquad u^h(x_i) \equiv u_i \neq \hat{u}_i ; \qquad x \in \Omega_s^x \qquad (5)$$

Where

$$\phi^T(x) = P^T(x)A^{-1}(x).B(x) \qquad (6)$$

And $\phi_i(x)$ is named as shape function, Where x corresponds to sample point of node i within the domain. The shape function is non-zero for a point within the support domain of node i this is known as compact support which is indispensible to preserve the local characteristic of the MLSAS. In the year 1998, Atluri [18] pointed out that the basis function's order and the weight function's type have strong effect on the smoothness of the shape function $\phi_i(x)$. The partial derivatives of such shape functions $\phi_i(x)$ as required for computation of strain were given by Belytschko [13].

In MLSAS, the linear and quadratic basis functions are implemented along with three weight functions popularly known as Spline weight function, Gaussian and Exponential weight function. Whereas Eq. (7) expresses spline weight function as

$$w(x-x_i)=\begin{cases}1-6\left(\frac{d_i}{r_i}\right)^2+8\left(\frac{d_i}{r_i}\right)^3-3\left(\frac{d_i}{r_i}\right)^4 & 0\le d_i\le r_i\\ 0 & d_i.>r_i\end{cases} \quad (7)$$

Where $w(x-x_i)$ is weight function; $d_i=|x-x_i|$ is the absolute distance between field node x_i and the point x. r_i is support domain radius for node i. It is worthwhile to mention here that the weight functions are defined only in support domain. The usefulness of said weight function was explained by Qing Xia Wang at el [36] and Jianfeng Ma [37]. The Gaussian weight function is presented through Eq. (8)

$$w(x-x_i)=\begin{cases}\left[\dfrac{\left\{e^{\left\{-\left(\frac{d_i}{C_i}\right)^{2k}\right\}}\right\}-\left\{e^{\left\{-\left(\frac{r_i}{C_i}\right)^{2k}\right\}}\right\}}{1-\left\{e^{\left\{-\left(\frac{r_i}{C_i}\right)^{2k}\right\}}\right\}}\right] & 0\le d_i\le r_i\\ 0 & d_i\ge r_i\end{cases} \quad (8)$$

Where C_i is a scaling parameter which controls the shape of the weight function and its effect on weight function was suggested by Thomas-Peter Fries [38].

It was also mentioned by Atluri [39] that the C_i value could be chosen arbitrary and the results are not a strong function of this C_i value. However, Liu [5] and Liu Kaiyuan [40] also explained on how to chose the value of C_i. In current implementation, the value of exponent k is taken as 1.

And the exponential weight function is expressed by Eq. (9) as under

$$w(x-x_i)=\begin{cases}e^{-\gamma\left(\frac{d_i}{r_i}\right)^2} & 0\le d_i\le r_i\\ 0 & d_i\ge r_i\end{cases} \quad (9)$$

Where γ is the smoothening parameter and its value can vary between 10^{-3} and 10^{3}. In year 2012 Abdollahifar [41] took the value of $\gamma=6$ to make the weight function bell shaped. The variation in test function with sub-domain radius r v/s γ scaling parameter for test function is presented through Fig. 2.

The value of smoothening parameter γ in the current implementation has been varied from 1 to 20 to examine the behavior of the exponential weight function. Now the formulation of elastic analysis of metal parts using modified meshless method is given as.

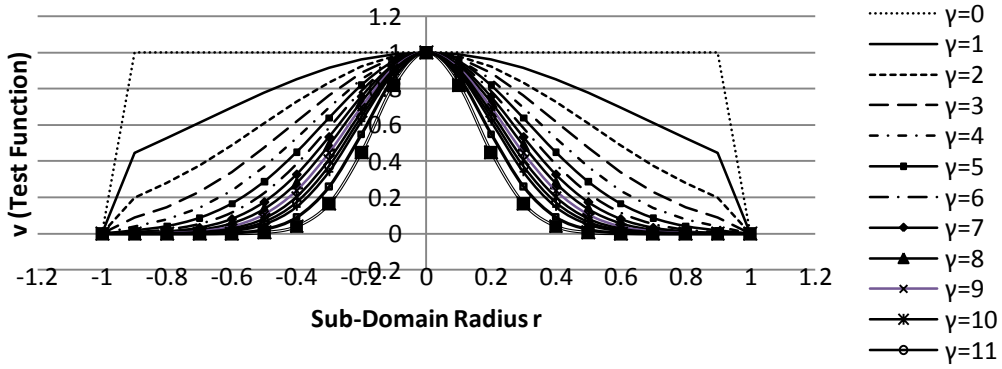

Fig: 2. Variation in Test Function with sub-domain radius r v/s γ scaling parameter for exponential test function

3. Formulation of Elastic Analysis Using Meshless Approach

On considering two dimensional region Ω, having boundary Γ and subjected to b_i body force as shown in Fig. 3. The schematic representation of global boundarieΓ, local boundaries Γ^p_{qi} or Γ^p_{qt} or Γ^p_{qu} or Γ^X_{qi} or Γ^p_q, global domain Ω, local sub-domains Ω_q, support domains Ω_s, boundary conditions Γ_u or Γ_t, domain of influence of a node *"i"*, domain of definition of a point *"f"* nodal discretization for 2-D case in truly meshless method is presented in Fig. 3. The following equilibrium equation Eq. (10) is generally utilized for elastic analysis.

$$\sigma_{ij,j} + b_i = 0 \qquad (10)$$

Where, $\sigma_{ij,j}$ represents the stress tensor partial derivative. The domain boundary Γ^p_u represents the portion of Γ. Here the essential boundary conditions for the p^{th} node are specified, and $u^p_i = \bar{u}^p_i$ holds. The Γ^p_t represents piece of Γ, where the natural boundary conditions are $\sigma_{ij}\mathcal{N}^p_j = \bar{t}^p_i$. The local unit normal vector at pth node that lies on the Γ_t boundary is $\mathcal{N}^p_j$. Atluri et al [42], Liu [43], and Abdollahifar et al [41] also applied this local weak form of equilibrium equation to a region bounded near p^{th} node as

$$\int_{\Omega^p_q} v^p_i\,(\sigma_{ij,j} + b_i)\,d\Omega = 0 \qquad (11)$$

Where Ω^p_q is the quadrature domain of p^{th} node. The quadrature domain could be any shape as specified by Cheng [44]. Moreover Eq. (11), v^p_i represent test function for p^{th} node. But Chyou-Chi Chien [45] stated that to make the formulation simpler, the test function should satisfy some of the properties like compactness, continuity and smoothness.

The local weak form as in Eq. (11) can be given for p^{th} node located within region Ω and on Γ boundaries i.e.

$$\Gamma^p_q = \Gamma^p_{qi} \cup \Gamma^p_{qu} \cup \Gamma^p_{qt} \qquad (12)$$

On substituting Eq. (12) in Eq. (11) and applying divergence theorem, the following Eq. (13) is now obtained.

$$\int_{\Gamma^p_{qt}} \sigma_{ij}\mathcal{N}^p_j\, v^p_i\, d\Gamma + \int_{\Gamma^p_{qu}} v^p_i\, \sigma_{ij}\mathcal{N}^p_j\, d\Gamma - \int_{\Gamma^p_{qi}} v^p_i\, \sigma_{ij}\mathcal{N}^p_j\, d\Gamma - \int_{\Omega^p_q} (v^p_{i,j}\sigma_{ij} - v^p_i b^p_i)\, d\Omega = 0 \qquad (13)$$

The Eq. (13) is valid for p^{th} node, where region is subjected to body force and a portion of boundary Γ is subjected to traction, and displacement boundary conditions are enforced.

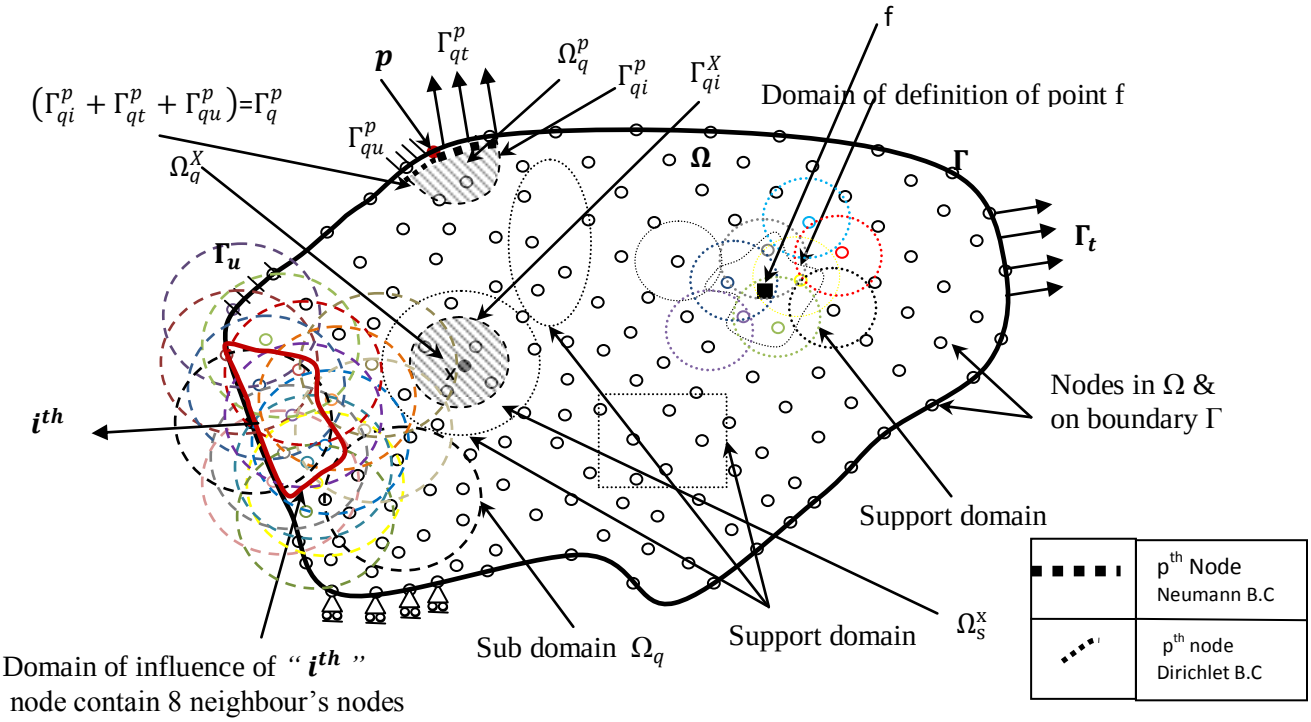

Figure 3:- Schematic representation of global boundaries Γ, local boundaries Γ^p_{qi} or Γ^p_{qt} or Γ^p_{qu} orΓ^X_{qi} orΓ^p_q , global domain Ω & local sub-domains Ω_q , support domains Ω_s, boundary conditions Γ_u or Γ_t ,domain of influence of a node "i", domain of definition of a point "f"; , nodal discretization for 2-D case in truly meshless method

The Eq. (13) can be deduced to Eq. (14) which is valid for all q^{th} nodes whose local boundaries do not interact with boundary Γ. And hence, the integral in Eq. (14) is being carried out over internal quadrature and integral over quadrature boundary Γ^q_{qi} vanishes. Because v^q_i test function is selected such that its value is zero at the boundary.

$$\int_{\Omega^q_q} (v^q_{i,j}\sigma_{ij} - v^q_i b^q_i)\, d\Omega = 0 \qquad (14)$$

In this formulation, the local weak forms given by Eq. (13) and (14) are applicable for continuous local domain

of p^{th} or q^{th} nodes. The continuum problem domain is now discretized into N finite nodes. The system equations contribution for all the N field nodes is being expressed by Eq. (15) in matrix form as under

$$[K]_{2N\times 2N}\{U\}_{2N\times 1} = \{F\}_{2N\times 1} \quad (15)$$

The solution of these 2N equations now provides nodal displacements for N field nodes along X and Y directions and can further be post processed to compute stresses and strains. In the above Eq.'s, the essential boundary conditions are enforced using direct interpolation method. For p^{th} field node, the essential boundary conditions are prescribed as $u_i^p = \bar{u}_i^p$ on Γ_{qu}^p boundary segment of Γ. The essential boundary conditions for p^{th} node can be applied through Eq. (15) just by replacing $(2p-1)^{th}$ and $(2p)^{th}$ rows of $[K]_{2N\times 2N}$ and $\{F\}_{2N\times 1}$matrix by $\sum_{i=1}^{NN}\phi_i^p$ and $\bar{u}_i^p$ respectively as suggested by Abdollahifar et al [41]. Where NN is number of nodes that lies within domain of influence of p^{th} node.

4. Validation of the Meshless formulation: Results and Discussion

Three case studies, namely first through an infinite plate with a central circular hole, second through thick cylinder subjected to internal pressure and third through an thin plate under normal loading are presented here for validating the said 2D Meshless formulation. These case studies are discussed as under.

4.1. Case study of an infinite plate with a central circular hole

An infinite plate with central circular hole subjected to unidirectional normal loading is considered for verifying the above presented meshless formulation treating plane stress case. A steel plate with central circular hole bearing the young's modulus of elasticity E = 210.8GPa, and Poisson's ratio $\nu = 0.3$, is subjected to normal traction along X direction of 1MPa. Due to symmetry in plate geometry, the loading and boundary conditions, the quarter segment of the plate is only considered for analysis as shown in Fig. 4. In the year 1987 Timoshenko [46] reported that when finite plate with circle hole having $\frac{r_w}{r_h} > 5$, then the solution is very close to that of an infinite plate with hole. Where r_w, the radial width of the plate is taken as 5m; r_h is the radius of circular hole which is 1m and length of quarter plate is 10m.

A comparison of $\|L_2\|$ error norm of normal stress σ_{xx} for different values of scaling parameter in exponential test functions both with linear and quadratic basis functions are shown in Fig. 4a & Fig 4b respectively. The close form solution of said case as given by Timoshenko [46] has been considered here, for the verification of results. The σ_{xx} stress distribution in the said plate loaded along X direction as obtained from the close form solution:

$$\sigma_{xx}(r,\theta) = P - P\left[\left(\frac{r_h}{r}\right)^2\left\{\frac{3}{2}\cos 2\theta + \cos 4\theta\right\}\right] + P\left\{\frac{3}{2}\left(\frac{r_h}{r}\right)^4\cos 4\theta\right\} \quad (16)$$

Where P, represents the traction force along X direction. The physical quarter plate with hole in present case is discretized non-uniformly into 443 nodes. The Gaussian test function replicated the stress field for σ_{xx} very well. Whereas, the computed results deviate for the other test functions. But, the error in computation could be minimized to a large degree, if the higher order basis functions are used.

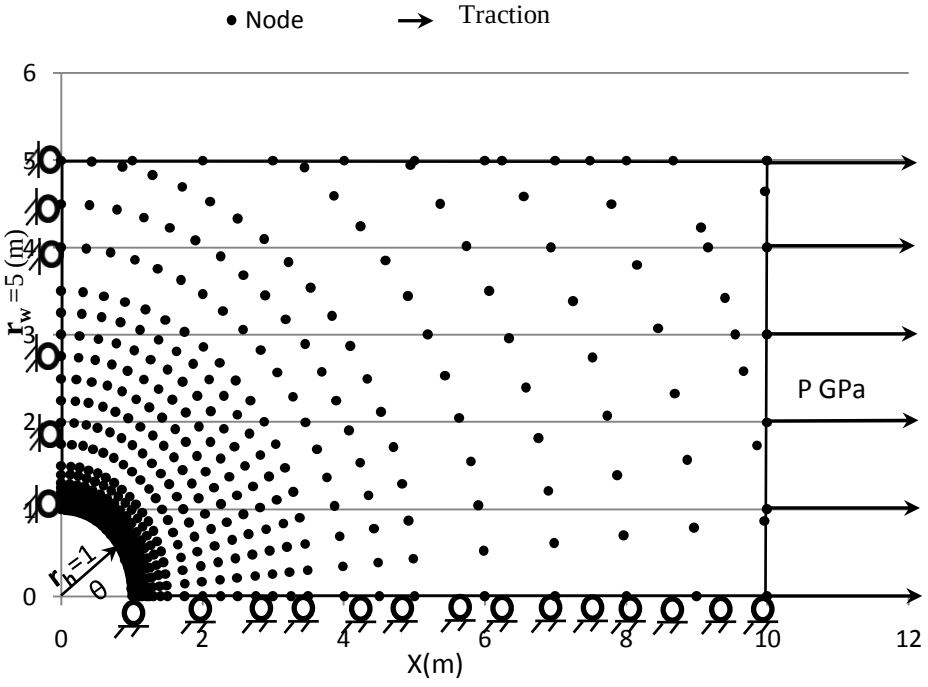

Fig: 4. Quarter infinite rectangular plate with circular hole nodal discretization, loading and boundary conditions

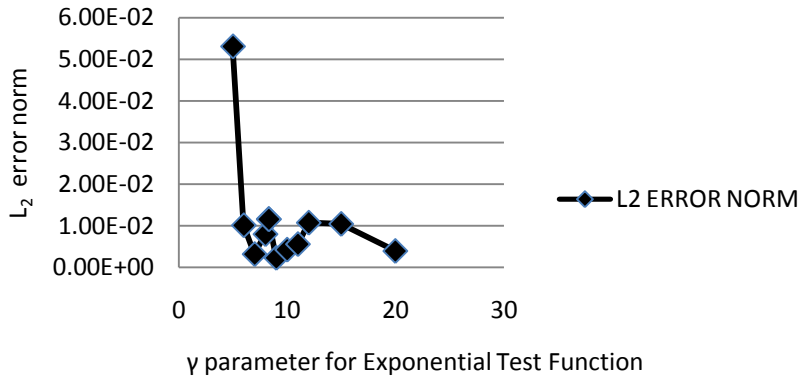

Fig: 4a. Comparison of $\|L_2\|$ error norm of σ_{xx} for different values of scaling parameter in exponential test functions with linear basis function

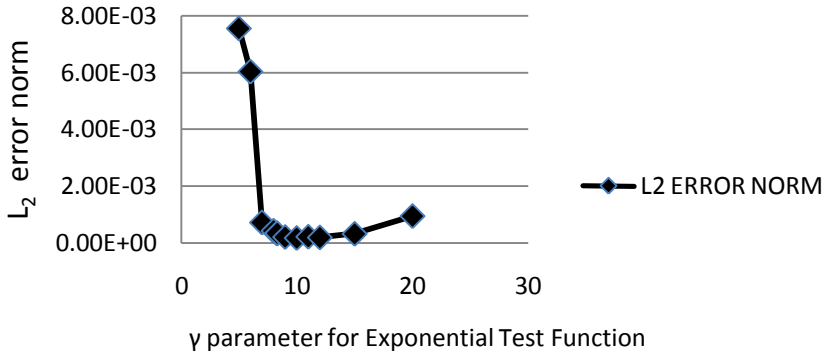

Fig: 4b. Comparison of $\|\mathbf{L_2}\|$ error norm of $\boldsymbol{\sigma_{xx}}$ for different values of scaling parameter in exponential test functions with quadratic basis function

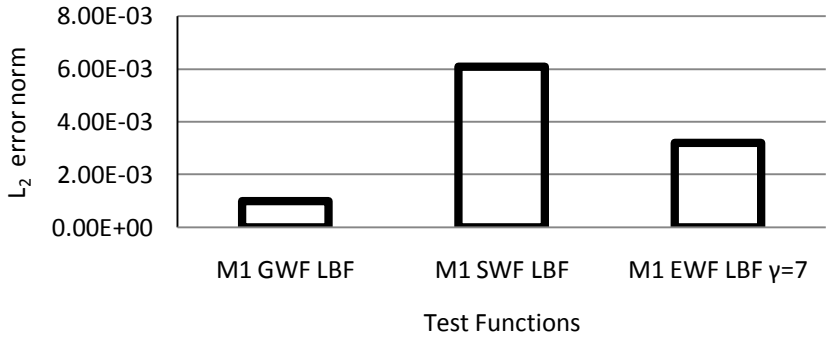

Fig: 4c. Comparison of $\|\mathbf{L_2}\|$ error norm of $\boldsymbol{\sigma_{xx}}$ for three different test functions with linear basis function

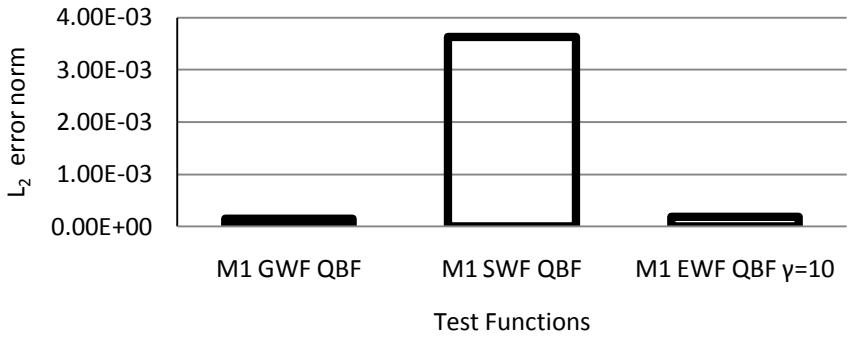

Fig: 4d. Comparison of $\|\mathbf{L_2}\|$ error norm of $\boldsymbol{\sigma_{xx}}$ for three different test functions with quadratic basis function

However, in order to study the impact of scaling factor γ, in the exponential test function, the variation of Euclidian norm is presented for different values of γ as shown in Fig. 4a with linear basis function and in Fig. 4b with quadratic basis function.

The magnitude of error can be minimized to a greater extent by suitably choosing the γ value in case of this current test function. It was also stated by Abdollahifar [**41**] that the suitable choice of this γ scaling parameter is more or less arbitrary. The scaling parameter γ as used in the exponential test function is tested for higher values. Bar charts are presented based on Euclidian norm for both the linear and quadratic basis function in Fig. 4c & Fig. 4d for all the three test functions. It is observed from these bar charts that the Euclidian norm is largest for Spline function, hence it gives worst results and the same was also observed by Ching [**47**] and Jianfeng [**37**] when the Gaussian and the spline functions are considered.

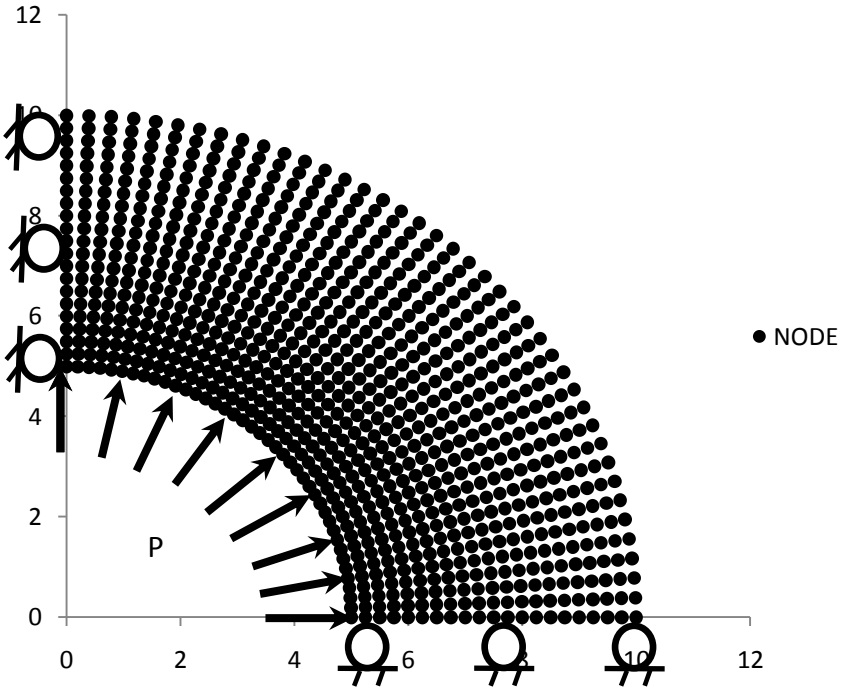

Fig: 5. Discretized geometry, boundary conditions and loading of cylinder

4.2. Case study of the thick cylinder subjected to internal pressure

The problem of the thick cylinder subjected to internal pressure is modeled as plane strain and is considered for validation. The steel cylinder with material properties as young's modulus of elasticity E=210.8GPa, Poisson's ratio $\upsilon = 0.3$, is subjected to an internal pressure 20 MPa. The geometry of the cylinder is such that it has an inner radius (R_i) 5m and outer radius (R_0) 10m, has the regular discretization with 861 field nodes. The discretization of the field nodes is such that 41 nodes are sprinkled along θ or circumference direction and 21 nodes along the radial direction.

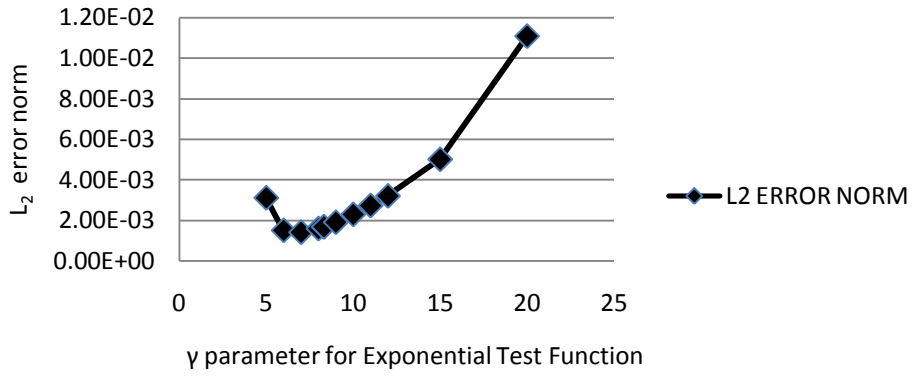

Fig: 5a. Comparison of $\|\mathbf{L_2}\|$ error norm of $\boldsymbol{\sigma_\theta}$ for different values of scaling parameter in exponential test functions with linear basis function

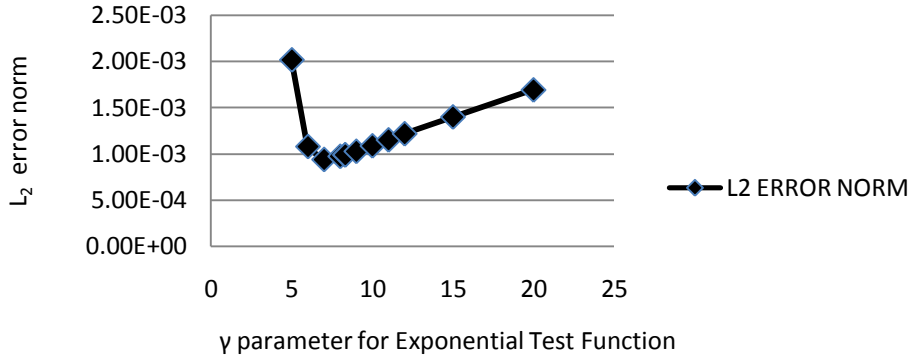

Fig: 5b. Comparison of $\|\mathbf{L_2}\|$error norm of $\boldsymbol{\sigma_\theta}$ for different values of scaling parameter in exponential test functions with quadratic basis function

Due to symmetries in the geometric and the loading conditions the upper right quadrant of cylinder is only considered in the current analysis. The discretized geometry, essential boundary conditions and the loading of the cylinder are as shown in Fig 5. The test function and the basis functions are same as in earlier problem. A comparison of $\|L_2\|$ error norm of the circumferential stress or the hoop stress (σ_θ) for the different values of the scaling parameter γ in exponential test functions are presented in Fig. 5a & Fig. 5b for both linear and quadratic basis functions respectively.

It can be construed from the bar charts shown in Fig. 5c & Fig. 5d that the results are in close agreement with FEM results for Gaussian and exponential test functions as they have least Euclidian error norm for both choices of the basis functions. And the spline function shows higher error norm for both choices of the basis functions. It could also be noticed from Figure 5a & Figure 5b, that the value of scaling parameter $\gamma = 7$ could be the optimal choice as it provides the best computational results for the current problem for both types of basis functions.

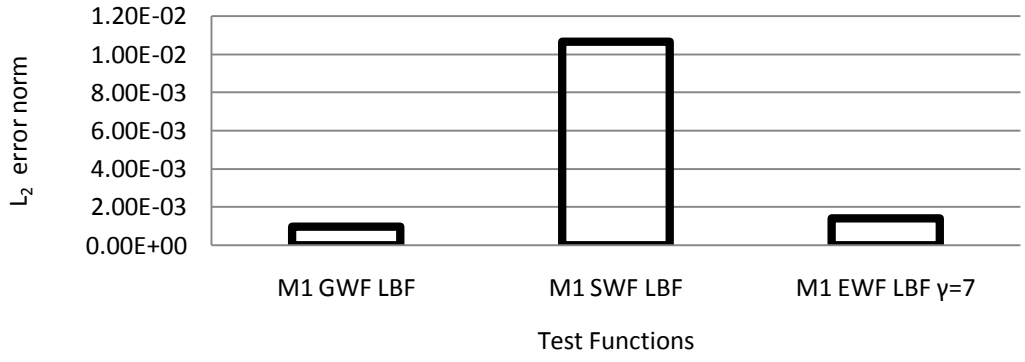

Fig: 5c. Comparison of $\|\mathbf{L_2}\|$ error norm of $\boldsymbol{\sigma_\theta}$ for three different test functions with linear basis function

Fig: 5d. Comparison of $\|\mathbf{L_2}\|$ error norm of $\boldsymbol{\sigma_\theta}$ for three different test functions with quadratic basis function

4.3 Case study of the thin plate under normal loading

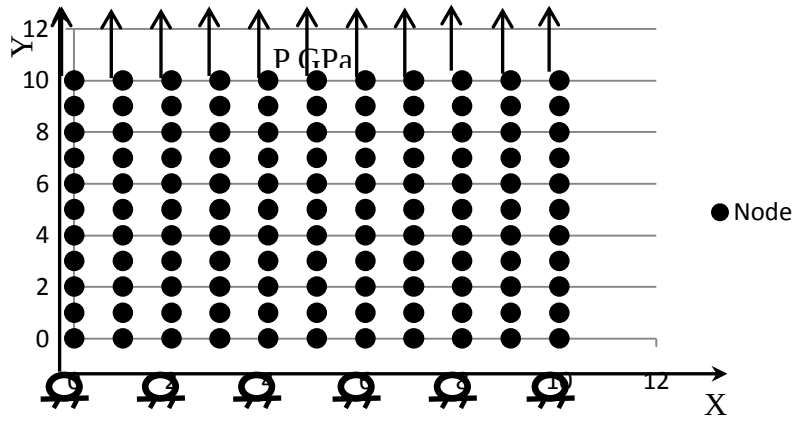

Fig: 6. Discretized geometry, boundary conditions and loading of thin plate

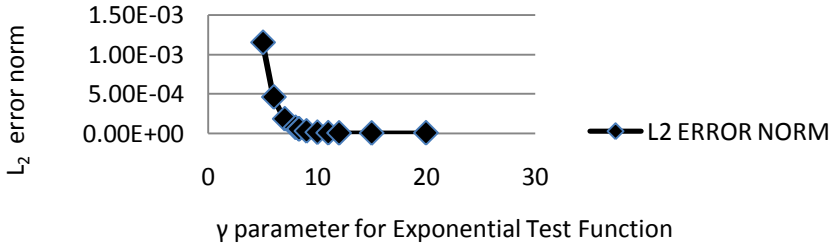

Fig: 6a. Comparison of $\|\mathbf{L_2}\|$error norm of $\boldsymbol{\sigma_{yy}}$ for different values of scaling parameter in exponential test functions with linear basis function

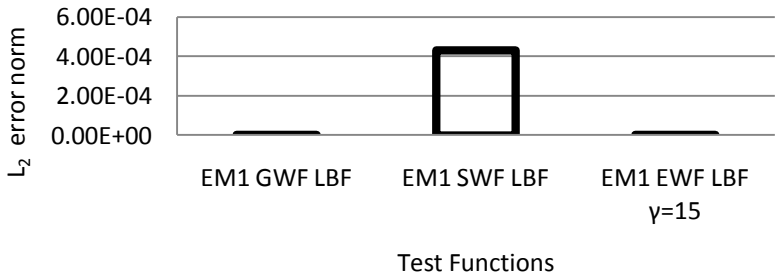

Fig: 6b. Comparison of $\|\mathbf{L_2}\|$error norm of $\boldsymbol{\sigma_{yy}}$ for different values of scaling parameter in exponential test functions with quadratic basis function

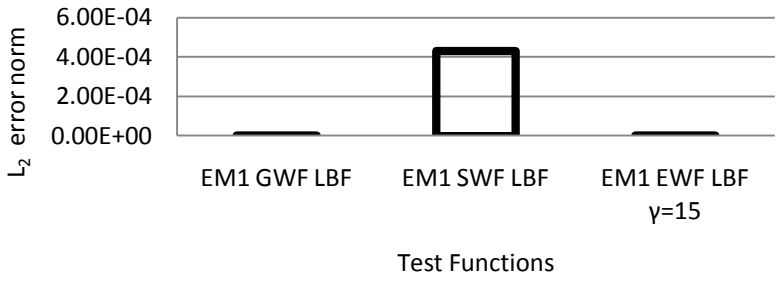

Fig: 6c. Comparison of $\|\mathbf{L_2}\|$ error norm of $\boldsymbol{\sigma_{yy}}$ for three different test functions with linear basis function

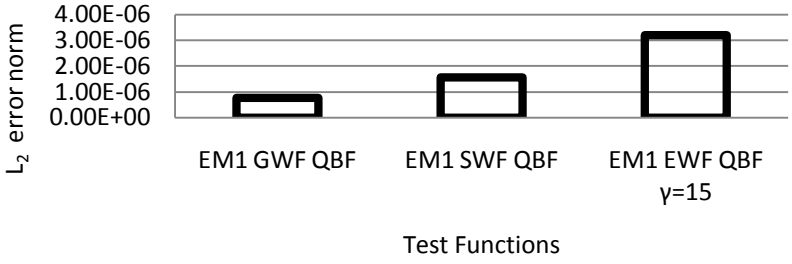

Figure 6d - Comparison of $\|\mathbf{L_2}\|$ error norm of $\boldsymbol{\sigma_{yy}}$ for three different test functions with quadratic basis function

To study the impact of scaling parameter γ for the exponential test function, the Euclidian error norm has been presented for the different values of γ as shown in Fig. 6a & Fig. 6b for both the linear and the quadratic basis functions. Gaussian test function simulated the stress field for σ_{yy} very close to analytical solution whereas for the other test functions a deviation was observed in the computed results. However, it could be seen from the bar charts as shown in Fig. 6c & Fig. 6d that the computational error can be reduced to a greater extent by implementing higher order basis functions. It can be observed form the Figs. 6c & 6d that the amount of error incurring in the computation can be lowered to a larger extent by suitable selection of scaling parameter γ in case of exponential test function. From Fig. 6d, it can be pointed out that for all cases presented above except for the thin plate with quadratic basis function the least Euclidian norm for exponential test function is not achieved within considered values of γ. However some other values can be tried so as to get closer results than spline test function. But owing to such a least error norm of order -6, it is quite unusual computationally to try for other γ values.

5. Conclusion

The current truly meshless approach is implemented for the three distinct test functions namely Gaussian, spline and exponential for solving elasticity problems. The above numerically solved cases illustrate that the nodal concentration, the order of basis function, the type of test function and the test function parameters all affect the numerical results. The appropriate choice of the test function parameters in Gaussian and exponential test function are observed significant and important in the present study. While in case of spline test function only the few parameters are chosen that made this function simpler to numerically implement and interpret. On the other hand, this feature of spline test function is at the cost of accuracy. The identical behavior of the spline test function is not only observed in the current implementation but also the same behavior was reported in the open literature that the Gaussian test function is better than the spline test functions and provides better results. It is not astonishing that the Gaussian test function provides the lowest Euclidian error norm and hence better accurate results, when compared against exponential and spline test functions. It is also worthwhile to mention here that in terms of accuracy, the Gaussian function provides accurate result while the exponential function yields better results for suitable choice of the parameters, and spline test function contribute to inferior results out of these three considered test functions.

The second prospective for comparing these test functions could be the choice of parameters to yield better accuracy in computation. It could be inferred from the above that the spline test function is affected by the least number of factors, whereas exponential test function needed a few more numbers of parameters in its characterization. While the Gaussian test function demands the largest number of variables in its characterization. It is very important to mention here that better results for Gaussian and exponential test functions are at the cost of suitably chosen parameters. The parameter dependent response of the exponential test function could be seen very clearly from the above graphs of γ parameter for Exponential Test Function v/s Euclidian error norm for both types of basis function. It is further suggested that there is no single value of scaling parameter that can provide best results. However, the γ parameter could be chosen from 7 to 15. It will also be important here to state here that even today the choice of

these test function parameters is arbitrary and experience based and still some modus operandi or procedure is required so that the optimum choice of these test function parameters can be made to make current approach more efficient.

The investigated case studies and open literature reveals that as the order of basis function is increased then the computational error can be minimized sufficiently. The bar charts for linear and quadratic basis function illustrates that for all the three test functions, the accuracy of the results is almost ten times better when the quadratic basis function is used over the linear basis function. It can be hence inferred from the above, that the choice of order of basis function has a significant effect whereas the test function's choice has relatively less influence on the accuracy of the solution.

It could be established from the above implementation that the solution of elasticity problem through meshless approach has strong dependence on nodal density, order of basis function and test function type. The order of basis function strongly influences the results as compared to test function type which is a strong function of optimum geometric parameters.

6. Acknowledgement

The support provided for this research by Dr. Atul Kumar Aggarwal, Associate Professor, Department of Mechanical Engineering, Delhi Technological University Delhi, India is highly acknowledged.

References

[1] S. S. Mulay, Li H., Meshless methods and their numerical properties. New york: CRC press, 2013

[2] S. Verma, N. Yadav, A. Chhillar, Dynamic analysis of a centelever beam using MLPG method, mechanical engineering, C.R. State College of Engineering, Sonipat ,India, 2006

[3] S. N. Atluri, The meshless method (MLPG) for domain & BIE discretizations. Forsyth, GA., USA: Tech science press, 2004

[4] S. Shen, S. N. Atluri, The Meshless Local Petrov-Galerkin (MLPG) Method.: Tech Science Press, 2002

[5] G. R. Liu, Meshfree methods moving beyond the Finite Element Method. Boca Raton, USA: CRC press, 2002

[6] M. B. Liu, G. R. Liu, Smooth partical hydrodynamics, a meshfree partical method. Toh Tuck Link, Singapore: world scientificpublication Co. Pte Ltd, 2003

[7] W. K. Liu, S. Li, Meshfree partical methods. Berlin, Germany: Springer, 2004

[8] Boogaard, Van den A. H., W. Quak, Nodal integration of meshless methods," in International confrence on Partical Based Method, Barcelona, 2009, 1-4

[9] P. Pudjisuryadi, Adaptive meshless local petrov-galerkin method with Variable domain of influence in 2D elastostatic problems, Civil engineering dimension, 10(2), 2008, 99-108

[10] D. Suvranu, K. J. Bathe, Towards an efficient meshless computational technique: the method of finite spheres, Engineering Computations, 18(1/2), 2001, 170-192

[11] J. J. Monaghan, R. A. Gingold, Smoothed particle hydrodynamics - Theory and application to non-spherical stars, Monthly Notices of the Royal Astronomical Society, 181, 1977, 375-389

[12] G. Touzot, P. Villon, B. Nayroles, Generalizing the Finite elemt method: diffuse approximation and diffuse elements., Computational Mechanics, 10(5), 1992, 307-318

[13] Y. Y. Lu, L. Gu, T. Belytschko, Element-free Galerkin methods., International Journal for Numerical Methods in Engineering, 37, 1994, 229-256

[14] Y. X. Mukherjee, S. Mukherjee, The Boundary Node Method for Potential Problems, International Journal for Numerical Methods in Engineering, 40(5), 1997, 797–815

[15] S. Jun, Y. F. Zhang, W. K. Liu, Reproducing kernel particle methods, International Journal for Numerical Methods in Fluids, 20(8-9), 1995, 1081-1106

[16] C. A. M. Duarte, Tworzydlo, T. J. Liszka, hp-Meshless cloud method, Computer Methods in Applied Mechanics and Engineering, 139, 1996, 263-288

[17] S. Idelsohn, O. C. Zienkiewicz, R. L. Taylor, E. Oñate, A finite point method in computational mechanics. Applications to convective transport and fluid flow, International Journal for Numerical Methods in Engineering, 39(22), 1996a, 3839-3866

[18] S. N. Atluri, T. Zhu, A new Meshless Local Petrov-Galerkin (MLPG) approach in computational mechanics, Computational Mechanics, 22, 1998, 117-127

[19] K. J. Bathe, S. De, The method of finite spheres, Computational Mechanics, 25, 2000, 329-45

[20] J. D. Zhang, S. N. Atluri, T. Zhu, A local boundary integral equation (LBIE) method in computational mechanics, and a meshless discretization approach, Computational Mechanics, 21, 1998b, 223-235

[21] Y. T. Gu., G. R. Liu, A point interpolation method for two-dimensional solids, International Journal for Numerical Methods in Engineering, 50, 2001, 937-951

[22] G. Xu, G. R Liu., A gradient smoothing method (GSM) for fluid dynamics problems, International Journal for Numerical Methods in Fluids, 58, 2008, 1101–1133

[23] P. Leinen, H. Yserentant, C. Gauger, The Finite Mass Method, Society for Industrial and Applied Mathematics Journal Numerical Analysis, 37(6), 2000, 1768–1799

[24] J. Zhang, H. Li, K. Y. Lam, B. T. Kee Bernard, G. R. Liu, Radial point interpolation based finite difference method for mechanics problems, International Journal for Numerical Methods in Engineering, 68(7), 2006, 728–754

[25] M. Ortiz, M. Arroyo, Local maximum-entropy approximation schemes: a seamless bridge between finite elements and meshfree methods, International Journal for Numerical Methods in Engineering, 65(13), 2006, 2167–2202

[26] Q. X. Wang, Li Hua, K. Y. Lam, A noval meshless approach- Local Kriging (LoKriging) method with two-dimentional structure analysis, Computational mechanics, 33(3), 2004, 235-244

[27] C. K. Park, The development of a generalized meshfree approximation for solid and fracture analysis, George Washington University, Washington, DC, Dissertation 2009

[28] M. Naisipour, J. Amani, M. H. Afshar, Node moving adaptive refinement strategy for planar elasticity problems using discrete least squares meshless method, Finite Elements in Analysis and Design, 47(12), 2011, 1315–1325

[29] V. Popov, E. H. Ooi, An efficient implementation of the radial basis integral equation method, Engineering Analysis with Boundary Elements, 36, 2012, 716–726

[30] L. Hua, K. Y. Lam, Q. X. Wang, Development of a new meshless — point weighted least-squares (PWLS) method for computational mechanics, Computational Mechanics, 35(3), 2005, 170-181

[31] W. A. Walker, The Repeated Replacement Method: A Pure Lagrangian Meshfree Method for Computational Fluid Dynamics, PLoS ONE: e39999., 7(7), 1-25, 2012

[32] S. Shen, S. N. Atluri, The basis of meshless domain discretization: the meshless local Petrov-Galerkin (MLPG) method, Advances in computational Mathematics, 3, 2005, 73-93

[33] P. Lancaster, K. Salkauskas, Surface generated by moving least square methods, Mathematics of Computation, 37(155), 1981, 141–158

[34] A. Rassineux, J. M. Savignat, P. Villon, P. Breitkopf, Efficient Solving of Mechanical Problem With Meshless Methods: Decomposition and Quadrature Scheme, Europpean congress on computational methods in applied sciences and engineering, 2000, 1-11

[35] A. Rassineux, P. Villon, P. Breitkopf, An Introduction to Moving Least Squares Meshfree Methods, Revue Européenne des Éléments, 11(7-8), 2002, 825-867

[36] L. Hua, K. Y. Lam, T. G. Yuan, Q. X. Wang, Analysis of Microelectromechanical Systems (Mems) by Meshless Local Kriging (Lokriging) Method, Journal of the Chinese Institute of Engineers, 27(4), 2004, 573-583

[37] J. Ma, Meshless Method for Modeling Large Deformation with Elastoplasticity, Mechanical Engineering, Kansas state University, Manhattan, Kansas, USA, Doctor of Philosophy Dissertation 2007

[38] H. G. Matthies, T. P. Fries, Classification and overview of meshfree methods, Department of Mathematics and Computer Science, Technical University Braunschweig, Brunswick, Germany, 2004

[39] T. L. Zhu, S. N. Atluri, A new meshless local petrove galerkin (MLPG) approach to Nonlinear problems in computer modeling and simulation, Computer modeling and simulation in engineering, 3, 1998, 187-196

[40] S. Long, G. Li, K. Liu, A simple and less-costly meshless local Petrov-Galerkin (MLPG) method for the dynamic fracture problem, Engineering Analysis with Boundary Elements, 30, 2006, 72-76

[41] M. R. Nami, A. R. Shafiei, A. Abdollahifar, A new MLPG method for elastostatic problems, Engineering Analysis with Boundary Elements, 36, 451-457, 2012.

[42] H. G. Kim, J. Y. Cho, S. N Atluri, A critical assessment of the truly meshless local Petrov-Galerkin (MLPG) and Local Boundary Integral Equation (LBIE) method., Computational Mechanics, 24, 1999b, 348-372

[43] Y. T. Gu, G. R. Liu, An Introduction to Meshfree Methods and their Programming. Netherland: Springer, 2005

[44] R. Cheng, Determination of a control parameter in a one dimensional parabolic equation using the moving least-square approximation, International Journal of Computer Mathematics, 85(9), 2008, 1363-1373

[45] C. C. Chyou, T. Y. Wu, An accurate solution to the meshless local petrov-galerkin formulation in elastodynamics, Journal of the Chinese Institute of Engineers, 27(4), 2004, 463-471

[46] J. N. Goodier, S. P Timoshenko, Theory of elasticity, 3rd ed. USA: MaGraw-Hill, 1987

[47] H. K. Ching, Solution of Linear Elastostatic and Elastodynamic Plane Problems by the Meshless Local Petrov-Galerkin Method, Engineering Mechanics, Virginia Polytechnic Institute and State University, Blacksburg, Virginia, Doctor of Philosophy Dissertation 2002